

# Residual Stress Relaxation Induced by Mass Transport Through Interface of the Pd/SrTiO<sub>3</sub>

S. Nazarpour · F. Afshar · C. Zamani ·  
N. Moghimian · A. Cirera

Received: 16 November 2009 / Accepted: 7 January 2010 / Published online: 20 January 2010  
© The Author(s) 2010. This article is published with open access at Springerlink.com

**Abstract** Metal interconnections having a small cross-section and short length can be subjected to very large mass transport due to the passing of high current densities. As a result, nonlinear diffusion and electromigration effects which may result in device failure and electrical instabilities may be manifested. Various thicknesses of Pd were deposited over SrTiO<sub>3</sub> substrate. Residual stress of the deposited film was evaluated by measuring the variation of d-spacing versus  $\sin^2\psi$  through conventional X-ray diffraction method. It has been found that the lattice misfit within film and substrate might be relaxed because of mass transport. Besides, the relation between residual intrinsic stress and oxygen diffusion through deposited film has been expressed. Consequently, appearance of oxide intermediate layer may adjust interfacial characteristics and suppress electrical conductivity by increasing electron scattering through metallic films.

**Keywords** Mass transport · Residual stress · Interfacial properties · Relaxation process

## Introduction

There is hardly an area related to thin film formation, properties, and performance that is uninfluenced by mass transport phenomena. This is especially true in microelectronic applications where very small lateral as well as depth dimensions of device features and film structures are involved. When these characteristic dimensions become comparable in magnitude to atomic diffusion lengths, compositional change could be expected. New phases in the form of precipitates, layered compounds, or even voids may be formed from ensuing reactions. These new phases can alter the initial film integrity through, for example, generation of stress or decreasing the adhesion. This, in turn, frequently leads to component and device malfunction and electrical instabilities manifested by decreases in conductivity as well as short- or even open-circuiting of conductors.

Residual stresses generally appear during the deposition of the thin films. Such stresses may lead to problems such as film detachment, bending of the system, and varying the interfacial properties. Therefore, evaluation of such interfacial stresses is of fundamental characteristics for metalization in microelectronic devices. The residual stress mainly consists of three kinds of stress; intrinsic, thermal, and external stress. Basically, residual stresses might be varied via substrate relaxation process [1], and essentially, substrate relaxation process occurs due to lattice misfit between the film and the substrate [2]. For that reason, it would be essential to concentrate on the variation of residual stress in different thicknesses of Pd film. Besides, by studying the variation of oxygen concentration on the interface of Pd/SrTiO<sub>3</sub>, it might be possible to reveal the correlation between residual stress and oxygen diffusion in the interface of Pd and SrTiO<sub>3</sub>.

---

S. Nazarpour · F. Afshar · C. Zamani · N. Moghimian ·  
A. Cirera  
MIND-IN2UB, Department of Electronics, Universitat de  
Barcelona, Barcelona 08028, Spain

S. Nazarpour (✉) · F. Afshar · C. Zamani · N. Moghimian ·  
A. Cirera  
UB, Department of Electronics, Universitat de Barcelona,  
Barcelona 08028, Spain  
e-mail: nazarpour@ub.edu

## Experimental Methods

The materials used in this study were 101B grade, both sides polished (100), oriented SrTiO<sub>3</sub> (STO) substrate, and 99.99% pure palladium. Electron beam evaporator was used for palladium evaporation. Graphite crucibles were employed for resistive evaporation. The evaporation chamber was pumped with mechanical and turbo molecular vacuum pump, while the base pressure of the chamber was  $4.7 \times 10^{-6}$  torr [1, 3].

Palladium was evaporated at 1.6 kV accelerating potential and 200 mA emission intensity for 20 min. Different STO substrates were positioned on the heater with different distances to evaporation source in order to obtain different thickness of Pd thin film [3]. Afterward, thicknesses varying from 10 to 100 nm with around 10-nm increment have been obtained with the substrate temperature kept on 300 °C.

The ex situ film thickness measurement has been done by means of Dektak 3,030 profilometer (Veeco). X-ray photoelectron spectroscopy (XPS) depth profiles were carried out to investigate the composition of the obtained films.

XPS data were collected in a Physical Electronics 5,500 spectrometer, working at a pressure of  $6 \times 10^{-9}$  torr. Aluminum K $\alpha$  X-ray was produced with a Physical Electronic X-ray source, which produce photons with an energy of 1,486.6 eV and natural line width of 0.9 eV. Data were fitted taking carbon 1 s orbital signal at 284.5 eV. To measure the oxygen concentration in the interface of STO, the ratio of the intensity of oxygen 1 s spectra between two points, one *near-interface* and another on the *interface*, was measured. *Near-interface* term refers to the area which Ti 2p concentration just starts to increase and *interface* term assumed to be the area in which the Ti 2p concentration is in the vicinity of its concentration in the substrate. Approximately, Ti 2p spectrum starts to appear around two nanometers away from interface. Simply, the ratio between these two terms (Fig. 1a the ratio between the intensity of point a and b) refers to oxygen 1 s concentration existed in the 2 nm above interface in the Pd film (point a in Fig. 1a) over the oxygen 1 s concentration in the interface (point b in Fig. 1a).

The crystalline structure has been determined by X-Ray Diffraction (XRD) analyses in  $\theta$ – $2\theta$  scan by means of a

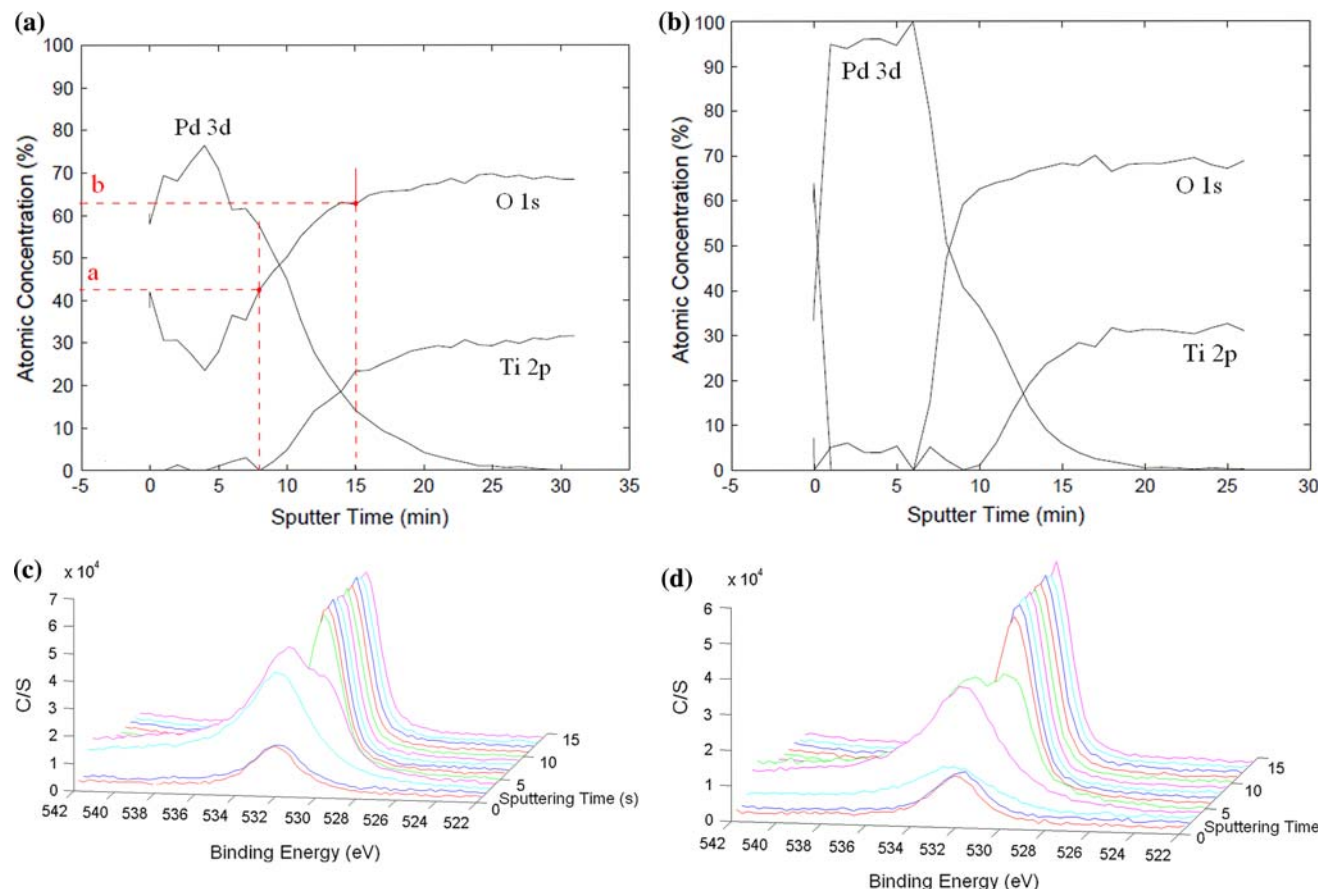
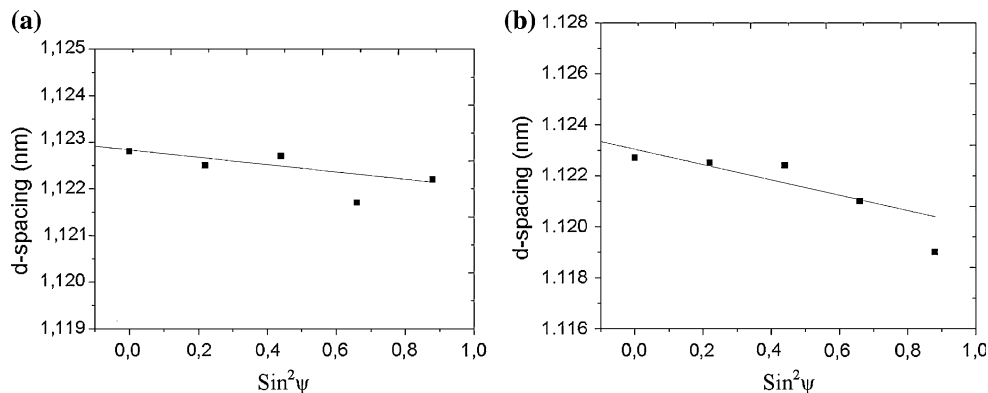


**Fig. 1** XPS in depth analysis of 30-nm (a) and 50-nm (b) Pd thin films deposited on SrTiO<sub>3</sub> perovskite substrate. a and b represent near-interface and interface terms which their ratio reveals simply the

percentage of diffused oxygen atoms from substrate through Pd film. c and d represent the in-depth variation of the oxygen 1s spectra for 30- and 50-nm Pd thin film

**Fig. 2** Plots of the d-spacing versus  $\sin^2\psi$  correspond to 30-nm (a) and 60-nm (b) Pd thin films. Schematic image in the Fig. 2a has been drawn to identify the  $\psi$  angle during measurement



4-circle X-ray diffractometer with Cu-K $\alpha$  radiation (MRD PHILIPS). Afterward, stress measurement was executed in  $\psi$ -tilt mode from around  $0^\circ$  to nearly  $180^\circ$  ( $2\theta = 80.5^\circ$ – $84.5^\circ$ ) in order to plot the d-spacing versus  $\sin^2\psi$ . Schematic representation of angle  $\psi$  was presented in Fig. 2a. Afterward with taking into account the poisson ration and elastic module [3], residual stress was measured for each Pd film [4, 5]. Besides, phase image of interface of Pd and STO were obtained by AFM, Digital Instruments Multimode—Veeco, in tapping mode ( $\nu = 300$  kHz) in order to reveal the intermediate layer.

## Discussion

Figure 1 represents XPS in depth analysis of Pd thin film deposited over STO. Accordingly, thin Pd film with 20 nm thickness exhibited negligible amount of oxygen atoms concentrated in the interface of the Pd films (Fig. 1a). In fact, the oxygen and Ti concentration increased similarly by increasing the sputtering time. This reveals the normal variation of elements from film toward substrate. From 50-nm Pd film shown in Fig. 1b, one can distinguish that when sputtering time reaches to 10 min (where it is essentially supposed to be empty from substrate elements) oxygen concentration is even higher than its concentration at substrate. Since the base pressure of the chamber was  $4.7 \times 10^{-6}$  torr, oxygen may not diffuse from the ambient. This anomalous behavior has been previously observed in Nazarpour et al. [1, 3, 6]. The top atomic layer of used STO substrate in this study consists of mainly Sr–O bonds. However, when the top atomic layer of STO is made of Ti–O bonds, presence of Oxygen in the interface has not been detected in any thickness of Pd thin film. Figure 1c and d correspond to variation of oxygen 1 s spectrum of 30 and 50 nm Pd thin films, respectively. High presence of oxygen in the interface of Pd and STO is significant. This oxygen has bounded to Pd and has different binding energies in the substrate. This is detected by the existence of two peaks in the interfacial region. This presence of

oxygen is in agreement with Fig. 1a, b which show the oxygen in the interface of Pd and STO.

It has been previously well established that at the nanoscale the intrinsic residual stress dominates the thermal stress, contrary to the macroscopic scale [7, 8]. Figure 2a, b show variation of Pd (222) crystal d-spacing versus  $\sin^2\psi$  for 30 and 60-nm Pd films, respectively. Obtained points fitted linearly in order to evaluate variation of residual strain in Pd (222) crystal direction. By considering elastic module and Poisson's ratio in each thickness [3], total amount of confined residual stress in the films may obtain, shown in Fig. 3. It can be seen that primarily experimental residual stress has fallen into a minimum at 30 nm. Afterward, the stress dramatically increased and reached to a plateau around 70 nm thickness. Although the Pd films are thin, standard deviations of residual stresses are significant, and the final trend would be comparable to Fig. 3. Variation of stress has been plotted regardless of the vector of stress. Essentially, stress is induced by external

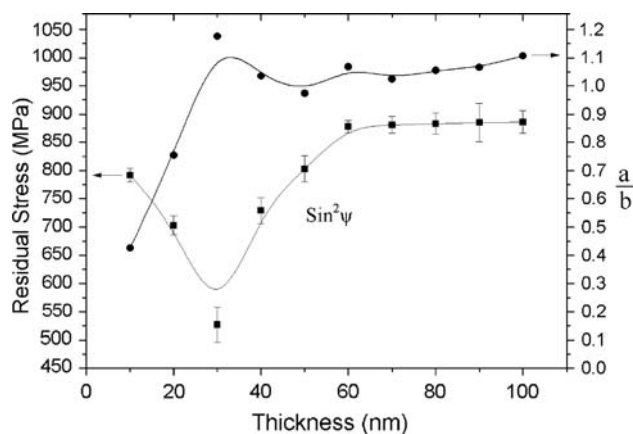


**Fig. 3** Experimental residual stress obtained by XRD (left perpendicular axis) and a/b ratio (right perpendicular axis) versus different thickness of Pd thin film. Point a refers to oxygen 1 s concentration existed in the 2 nm above interface in the Pd film and point b corresponds to the oxygen 1 s concentration in the interface, see Fig. 1a. Correlation between two plots is attributed to oxygen diffusion through Pd film which caused by relaxation process

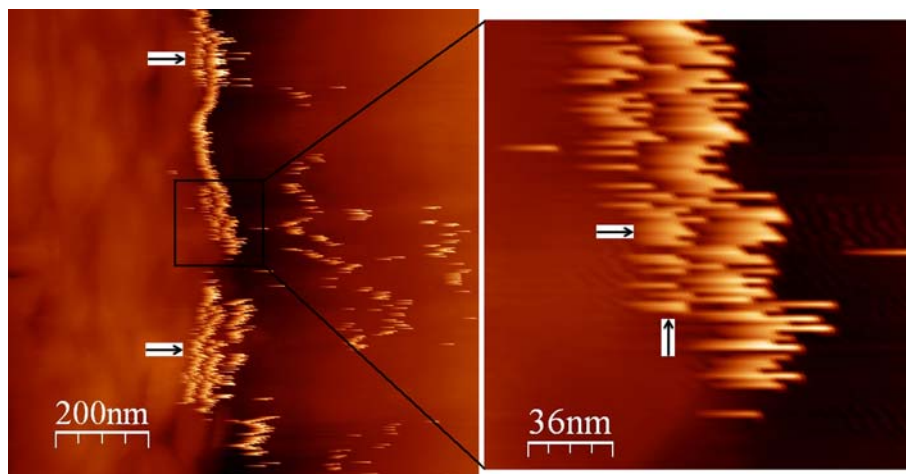
factors during the application process, but it is also an intrinsic property which is already generated during film growth [9–11]. Based on our previous studies [1], the growth of Pd over STO follows the Stranski–Krastanow growth mode where 3D islands nucleate on top of a thin wetting layer. Besides, in the case of high melting temperature film, the ad-atom mobility is assumed to be quite limited, however, raising the deposition temperature from room temperature to 300 °C, transforms the growth mode from that of a low mobility metal to the high mobility ones. Aberman [12] reported that evaporated polycrystalline metal films grow by one of the two mechanisms: low mobility or high mobility Volmer-Weber mode, each characterized by specific morphology and stress behavior. Since it has been proved that polycrystalline Pd film grows layer by layer during the deposited first atomic layers, its stress variation in higher thicknesses might be adapted by Aberman theories which are based on Volmer-Weber growth. The compressive stress in high mobility, continuous and Volmer-Weber films originates from compressive strain built up in the pre-coalescence stage [13] where the films still consists of isolated islands. Due to Laplace pressure, the lattice spacing in islands is smaller than in the bulk [14] and converges to the bulk value upon island growth. The lattice parameter of bulk STO is 0.390 nm and for bulk Pd is 0.389. However, this lattice misfit intensifies by decreasing the dimension of Pd from bulk to nanometric thin film. Calculated lattice misfit of 30 nm Pd thin film is 0.384 nm [1]. Therefore, it might be assumed that oxygen atoms may penetrate into Pd film in order to compensate the intensified lattice misfit within Pd and STO. Figure 3 points out this important fact that large percentage lattice misfit may lead to mass transfer from substrate through deposited film in order to relief residual intrinsic stresses. Presence of oxygen in the interface of some thickness of Pd film such as 30, 60, and 100 nm is dramatically higher than oxygen concentration in the perovskite substrate.

Although parameters such as melting point of deposited material, porosity of deposited film, and substrate temperature during deposition may play effective roles and modify this oxygen diffusion. Mass transport between films and their substrate strongly restricts the application of metallic films by intensifying the electron scattering in the film. Additionally, oxide intermediate layer may change interfacial electrical properties which, for instance in capacitor applications, increases the loss of the dielectric layer. Besides, this oxide intermediate layer diminishes the sharp interface between film and substrate. To study the interface, AFM phase image were obtained from interface (cross-section) of 30 nm thin Pd film deposited over STO perovskite substrate, shown in Fig. 4. The area in the left of the Pd film (shiny line) corresponds to substrate, and the right part of this line is artifact due to tip dimension. In some areas, film did not cover the substrate or was not detected by tip due to low thickness of Pd film. However, some regions that consist of extra layers within film and substrate are detected that can be seen in the magnified image. It could be suggested that this layers attributed to oxide intermediate layer which appeared because of the presence of oxygen in the Pd film (shown by arrows in Fig. 4). In addition, it could be concluded from Fig. 4 that sharp interface is sacrificed due to residual stress relaxation which is not favorable in the microelectronic technology.

## Conclusion

Initially, it is found that oxygen diffusion from substrate into the Pd thin films occurs which leads to an intermediate oxide layer between Pd and STO. Besides, relation between the residual stresses and oxygen concentration in the interface reveals that oxygen penetrates into Pd film to compensate lattice misfit between film and substrate. Therefore, it could be concluded that mass transport could even appear because

**Fig. 4** AFM phase image of the 30-nm Pd film deposited over STO. Left area of the thin film (*shiny line*) is related to substrate, whereas right part is artifact caused by tip dimensions



of residual stresses in the thin films. This, in turn, drastically influences desired properties in the microelectronic technology. Mass transport frequently leads to component and device malfunction and electrical instabilities manifested by decreases in conductivity as well as short- or even open-circuiting of conductors. This study reveals the importance of deep and cutting edge further studies on mass transport caused by residual stresses.

**Open Access** This article is distributed under the terms of the Creative Commons Attribution Noncommercial License which permits any noncommercial use, distribution, and reproduction in any medium, provided the original author(s) and source are credited.

## References

1. S. Nazarpour, E. Langenberg, O. Jambois, C. Ferrater, M.V. Garcia-Quenca, M.C. Polo, M. Varela, *Appl. Surf. Sci.* **255**, 3618 (2009)
2. M. Ohring, *Material science of thin films*, 1st edn. (Academic Press, San Diego, 1992)
3. S. Nazarpour, C. Zamani, A. Cirera, *Appl. Surf. Sci.* **255**, 8995 (2009)
4. G.C.A.M. Janssen, A.J. Dammers, V.G.M. Sivel, W.R. Wang, *Appl. Phys. Lett.* **83**, 3287 (2003)
5. G.C.A.M. Janssen, J.D. Kaminga, *Appl. Phys. Lett.* **85**, 3086 (2004)
6. S. Nazarpour, A. Cirera, O. Jambois, C. Ferrater, M.V. Garcia-Quenca, M.C. Polo, M. Varela, *J Nanosci. Nanotechnol.* **10**, 2635 (2010)
7. G. Guisbiers, O. Van Overschelde, M. Wautelet, *Acta Mater.* **55**, 3541 (2007)
8. G. Guisbiers, M. Wautelet, L. Buchailot, *Sripta Mater.* **60**, 419 (2009)
9. G. Hass, R.E. Thun, *Physics of thin films*, vol. 3 (Academic press, New York, 1966), p. 211
10. M.F. Doerner, W.D. Nix, *CRC crit. Rev. Solid State Mater. Sci.* **14**, 225 (1988)
11. R. Koch, *J. Phys.: Condens. Matter* **6**, 9519 (1994)
12. R. Abermann, *Vacuum* **41**, 1279 (1990)
13. R. Abermann, R. Koch, R. Kramer, *Thin Solid Films* **58**, 365 (1979)
14. C.W. Mays, J.S. Vermaak, D. Kuhlmann-wilsdorf, *Surf. Sci.* **12**, 134 (1968)